Physics Scholarship   Physics

Revisiting two-step Forbush decreases

Andrew P. Jordan
University of New Hampshire, A.P.Jordan@unh.edu

Harlan E. Spence
University of New Hampshire, harlan.spence@unh.edu

J. B. Blake

D. N. A. Shaul

Recommended Citation

Jordan, A. P., H. E. Spence, J. B. Blake, and D. N. A. Shaul (2011), Revisiting two-step Forbush decreases, J. Geophys. Res., 116, A11103, doi:10.1029/2011JA016791.

Revisiting two-step Forbush decreases

A. P. Jordan,[1] H. E. Spence,[1] J. B. Blake,[2] and D. N. A. Shaul[3]

[1]   Interplanetary coronal mass ejections (ICMEs) and their shocks can sweep out galactic cosmic rays (GCRs), thus creating Forbush decreases (FDs). The traditional model of FDs predicts that an ICME and its shock decrease the GCR intensity in a two-step profile. This model, however, has been the focus of little testing. Thus, our goal is to discover whether a passing ICME and its shock inevitably lead to a two-step FD, as predicted by the model. We use cosmic ray data from 14 neutron monitors and, when possible, high time resolution GCR data from the spacecraft International Gamma Ray Astrophysical Laboratory (INTEGRAL). We analyze 233 ICMEs that should have created two-step FDs. Of these, only 80 created FDs, and only 13 created two-step FDs. FDs are thus less common than predicted by the model. The majority of events indicates that profiles of FDs are more complicated, particularly within the ICME sheath, than predicted by the model. We conclude that the traditional model of FDs as having one or two steps should be discarded. We also conclude that generally ignored small-scale interplanetary magnetic field structure can contribute to the observed variety of FD profiles.

Citation: Jordan, A. P., H. E. Spence, J. B. Blake, and D. N. A. Shaul (2011), Revisiting two-step Forbush decreases, *J. Geophys. Res.*, *116*, A11103, doi:10.1029/2011JA016791.

1.   Introduction

1.1.   Motivation

[2]   Galactic cosmic rays (GCRs), which are relativistic charged particles, fill interplanetary space. (Some researchers include a neutral component, i.e., gamma rays, in the term cosmic rays; in this paper, however, the term refers only to the charged component.) The Sun's interplanetary magnetic field (IMF) modulates these particles on a broad range of size scales, from those comparable to the heliosphere to those of only a hundred megameters. One of the most dramatic modulations occurs when the Sun ejects large (0.3 AU in the radial direction, on average), coherent magnetic structures called interplanetary coronal mass ejections (ICMEs). An ICME is a large magnetic loop generally anchored to the Sun. As it travels through the heliosphere, the ICME and its shock, if present, sweep out cosmic rays. This reduction in cosmic ray intensity is called a Forbush decrease (FD). Such an event can sometimes decrease the intensity of GCRs at 1 AU by as much as 20%.

[3]   The traditional model of FDs predicts that an ICME and its shock decrease the GCR intensity in a two-step profile. As we show below, however, this view has been the focus of little testing. Thus, our goal is to discover whether a passing ICME and its shock inevitably lead to a two-step FD, as predicted by the model.

[4]   The answer to this question will serve two purposes. First, it will help disclose the nature of the sheath between an ICME and its shock. Because the sheath comprises shocked IMF, understanding it will in turn help us better understand the nature of the ambient IMF. Second, learning how the sheath affects cosmic rays will also improve our knowledge of energetic particle transport in the IMF. Thus, this study will improve our knowledge of both the transport of GCRs and the medium of that transport. We first start by tracing the history of the FD model to show its limitations.

1.2.   History of the FD Model

[5]   *Forbush* [1937] was the first to observe a geomagnetic storm that was concurrent with a decrease in GCR fluxes measured on the ground. Further work showed that an external driver was responsible for both a storm and its associated FD [*Simpson*, 1954]. Two years later, *Morrison* [1956] posited that a plasma cloud ejected from the Sun could drive such a decrease. In 1960, data from the Pioneer V spacecraft en route to Venus confirmed this idea. The combination of in situ IMF and GCR measurements conclusively showed that interplanetary disturbances were responsible for the cosmic ray decrease [*Coleman et al.*, 1960; *Fan et al.*, 1960]. For a further summary of early work on FDs, see the review by *Lockwood* [1971].

[6]   *Barnden* [1973] was the first to identify two-step FDs. The author presented five such events from the years 1966 to 1972. He hypothesized that their profiles resulted from the effects of both the shock and its driver. In this model, the shock created the first step of such events, and the tangential

---

[1]Institute for the Study of Earth, Oceans, and Space, University of New Hampshire, Durham, New Hampshire, USA.
[2]The Aerospace Corporation, El Segundo, California, USA.
[3]High Energy Physics Group, Department of Physics, Imperial College London, London, UK.

discontinuity at the leading edge of the driver created the second step.

[7] The hourly-averaged IMF data he used, however, likely hampered his ability to identify the arrival of the driver. Also, the author only searched for two-step decreases in the GCR data. He did not look for interplanetary disturbances that could lead two-step FDs, as predicted by the model. Therefore the study left open the question of whether every shock and its driver create a two-step FD.

[8] *Sanderson et al.* [1990] conducted the next major study of two-step FDs. At that time, some confusion existed about whether magnetic clouds (ICMEs with strong flux rope signatures) or their accompanying shocks create the cosmic ray decreases. The authors analyzed 19 magnetic clouds associated with GCR decreases of at least 2%.

[9] On each event they superimposed an idealized two-step FD profile [see *Sanderson et al.*, 1990, Figure 1a]. They measured both the time from the shock to the first GCR minimum and the time from the arrival of the magnetic cloud to the second GCR minimum. The authors concluded that the shock and sheath create a thick slab diffusive barrier against the cosmic rays. That is, the barrier continues throughout the sheath. They decided that a thin slab barrier, i.e., the tangential discontinuity at the leading edge of the magnetic cloud, drives the second step.

[10] There are a few important points regarding this analysis. First, the authors used only one neutron monitor. Identifying small features using a single, low geomagnetic latitude monitor is difficult because of diurnal variations and other anisotropic features. Second, they assumed that applying the two-step profile was correct in every event, which is different from testing the validity of the profile. Figure 2 of *Sanderson et al.* [1990] shows this most clearly: the two-step profile is unable to fit five of the eight largest events they show. Furthermore, their model of a thick barrier continuing through the sheath is unable to account for local recovery shown in the idealized situation in Figure 1a of *Sanderson et al.* [1990].

[11] A few years later, *Cane* [1993] concluded that both the turbulence in the sheath and the enhanced magnetic field of the magnetic cloud can decrease GCRs. The study combined ground- and space-based GCR data. The purpose of the analysis was to differentiate between the effects of the shock and of the magnetic cloud, not to test explicitly the two-step profile.

[12] This study continued in two later papers [*Cane et al.*, 1993, 1996]. The authors divide cosmic ray decreases into four classes. They base these classes on the characteristics of the interplanetary medium (IPM), not the GCR decrease profile. The first class is accompanied by a shock and ICME, the second by only a shock, the third by an ICME with a weaker shock, and the fourth by multiple disturbances. The authors identify the various magnetic structures by observing IMP 8 particle data with a relatively low threshold (>60 MeV/amu ions). They also use hourly-averaged interplanetary data when available (for about half the events in the second paper). In the more comprehensive second paper, they find 153 cosmic ray decreases from 1964 to 1994. Eighty-six percent of the events coincide with an ICME and its shock. That is, they fall into either the first or third class, both of which the authors explicitly equate with two-step FDs.

[13] In both these studies, the authors focus on whether a decrease occurred, not whether it had a step at the shock and another at the leading edge of the ICME. In other words, they assume two-step FDs occur when both ICMEs and their shocks are present. An example of this can be seen in Figure 5 of *Cane et al.* [1993]. It shows a decrease that began during the ICME rather than at the shock; the event is not a two-step FD. While the authors note that the decrease began at the ICME and not at the shock, they still identify the event as belonging to the third class, which comprises two-step FDs.

[14] *Cane et al.* [1994] did a related and important analysis using three spacecraft to observe events from widely spaced locations. Their spacecraft data (>60 MeV/amu ions) are from IMP 8 and Helios 1 and 2. These data lack the potentially large diurnal variations found in neutron monitor data. The authors conclude that ICMEs create local and abrupt cosmic ray decreases, whereas the shock is nonlocal and drives a more gradual decrease and recovery longer than does the ICME.

[15] Their conclusion, however, appears unable to explain what they consider to be their clearest event. In the data from all three spacecraft, the GCR intensity rapidly decreases for a few hours after the shock and then decreases more slowly further in the sheath [see *Cane et al.*, 1994, Figures 2 and 13]. That initial small but rapid decrease appears to contradict their conclusion that the shock creates a gradual decrease in cosmic rays. Also, the ICME-related steps are only apparent because the GCR intensity begins to level after the initial decrease. For example, in Figure 13 of *Cane et al.* [1994], the initial decrease at the shock has approximately the same slope as the ICME-driven decrease in the Helios 2 data. Thus, if the ICME had occurred about 12 h earlier (that is, before the leveling between the two steps), resolving the two steps would be difficult. The question remains, then, of why the slope of the GCR intensity changes so quickly within the sheath.

[16] *Wibberenz et al.* [1998] outline the only model of FDs that takes into account the two regions that modulate cosmic rays (see also the excellent review of FDs by *Cane* [2000]). In this model, the ICME's shock drives a gradual decrease that continues throughout the sheath. This decrease can result from a variety of factors. First, the increase in solar wind speed increases convection and adiabatic cooling of the cosmic rays in the sheath. Second, enhanced turbulence and possible changes in magnetic topology affect the diffusion of cosmic rays. Finally, the increased field strength in the sheath reduces drifts into the sheath. Unlike the shock, the ICME creates only a local decrease by its leading tangential discontinuity and subsequent closed field lines. After it passes, the recovery is due to the shock effect. In Figure 1 of *Wibberenz et al.* [1998], they show how the two components of the decrease fit two FDs. As can be seen in the figure, though, this model is unable to explain the leveling in the GCR data immediately prior to the arrival of the ICMEs. Something else in the IMF likely plays a role, as well.

1.3. Weaknesses of the FD Model

[17] The above studies agree that two different phenomena contribute to FDs: the shock and the ICME. The first step of the FD begins at the shock and continues into the sheath. The second step begins at the tangential discontinuity at the ICME's leading edge [*Cane*, 2000]. Therefore if only a shock

Table 1. Neutron Monitors

Station	Latitude	Longitude	Altitude (m)	Vertical Cutoff Rigidity (GV)	Scaling Factor
Inuvik	68.35	−133.72	21	0.16	100.0
Climax	39.37	−106.18	3400	2.97	100.0
Newark	39.70	−75.70	50	2.02	100.0
Thule	76.50	−68.70	44	0.00	100.0
Sanae	−71.67	−2.85	856	0.73	100.0
Kiel	54.30	10.10	54	2.29	100.0
Oulu	65.06	25.47	15	0.77	100.0
Apatity	67.55	33.33	177	0.60	64.0
Moscow	55.47	37.32	200	2.43	64.0
Norilsk	69.29	88.05	0	0.58	64.0
Irkutsk	52.47	104.03	435	3.64	100.0
Cape Schmidt	68.55	180.32	0	0.45	64.0
McMurdo	−77.90	166.60	48	0.00	100.0
South Pole	−90.00	0.00	2820	0.09	100.0

or an ICME encounters the cosmic ray detector, the data will instead show a FD with a single step.

[18] The two-step profile has remained untested. Some of the above analyses show some events that appear to be two-step FDs, but the events are shown without IPM data. Some studies indicate that both the sheaths of ICMEs and the ICMEs themselves decrease the intensity of cosmic rays. These studies do not show, however, whether the combination of the two effects will create two steps, as first defined by *Barnden* [1973]. Furthermore, the observed leveling of the GCR intensity between the steps remains unexplained. As *Cane* [2000] indicates, no comprehensive study has yet taken into account both steps.

[19] This gap in the understanding of FDs must be filled. Doing so will give us better knowledge of the nature of the IMF during disturbed conditions and how energetic particles propagate through it. The simplest way to test the traditional understanding is to identify periods when the interplanetary conditions are conducive to creating two-step FDs. If the model is correct, then such periods will typically coincide with two-step FDs.

2. Data Sources

[20] Two factors inhibited the above studies from testing whether ICMEs and their shocks necessarily drive two-step FDs. First, some studies did not examine the GCR profile in detail. This was sometimes due to using only one or two neutron monitors. Diurnal and other anisotropic variations can make identifying steps difficult. Also, some studies only considered the occurrence of a decrease and not its profile. These thus missed the chance to test conclusively whether two steps commonly occur. Second, other studies did not examine the details of the IPM data. This was sometimes due to the lack of adequately high time resolution, which made distinguishing between the sheath and the ICME difficult. Therefore properly exploring the connection between ICMEs and two-step FDs requires the use of many neutron monitors; spacecraft data, if available; and high time resolution IPM data.

[21] We use cosmic ray data from 14 neutron monitors around the world: Inuvik, Climax, Newark, Thule, Sanae, Kiel, Oulu, Apatity, Moscow, Norilsk, Irkutsk, Cape Schmidt, McMurdo, and South Pole. (For a description of neutron monitors, see *Simpson* [2000].) Their properties are listed in Table 1. The sixth column shows the conversion factor from the data we show below to counts per hour. They are spread in longitude for easy identification of anisotropic features, such as diurnal variations. The monitors at Thule and McMurdo are close enough to the geomagnetic poles to have generally little diurnal variation. The neutron monitors closest to the poles measure particles with rigidities of $\gtrsim 1$ GV, which, for protons, correspond to energies greater than or equal to 500 MeV. The gyroradius of such a particle in a 5 nT field is about 5×10^5 km. The other monitors detect particles with higher rigidities.

[22] The studies mentioned in the introduction typically had the limitation of using only one or two neutron monitors. Doing so introduces a large uncertainty as to when features in the cosmic ray profile, such as the onset of a decrease, occur. Diurnal variations and anisotropies in the cosmic rays create this uncertainty and inhibit the identification of global features. By using data from many neutron monitors, we can easily identify diurnal or anisotropic features.

[23] We also use, when possible, GCR data from the spacecraft INTEGRAL (International Gamma Ray Astrophysical Laboratory). The spacecraft launched on 17 October 2002. Its 3 day orbit has an apogee of ~24 R_E, a perigee of ~1.4 R_E, and an inclination of 51.6 degrees. The purpose of the high apogee is to minimize the time INTEGRAL spends within the Earth's radiation belts. Thus, the spacecraft is outside the magnetosphere for much of its orbit.

[24] The spacecraft carries an instrument called the Spectrometer for INTEGRAL (SPI). SPI contains an array of 19 germanium crystals that detect gamma rays. GCRs of energies $\gtrsim 200$ MeV (gyroradii of 4×10^5 km in a 5 nT magnetic field) can penetrate the spacecraft and saturate the detector. An onboard computer records the saturating events, which we use as cosmic ray data. Thus, the data are essentially from an integral energy channel. For a more detailed description of using the instrument to detect cosmic rays, see *Jordan et al.* [2009].

[25] SPI is an excellent monitor of GCRs. The detector has a field of view of about 4π sr. Because of the instrument's large geometric factor (roughly 18,000 cm^2 sr), it counts GCRs at a rate of about 4000 ct/s. The good counting statistics enable exploration of short time scale features in the cosmic ray time series (we show 10 min resolution data throughout this paper). Also, since the spacecraft is usually outside the magnetosphere, it does not suffer from diurnal variations that can overwhelm GCR features because of IPM variations. Since radiation belts particles and solar energetic particles overwhelm the GCR signal, we remove data when either population is present.

[26] The Advanced Composition Explorer (ACE) spacecraft provides the IPM data we use. The ACE Magnetic Field Experiment (MAG) became operational on 2 September 1997, and the Solar Wind Electron Proton Alpha Monitor (SWEPAM) on 4 February 1998. When solar wind velocity data are available, we ballistically propagate the data from the spacecraft to Earth. We do so by assuming a constant velocity component along the Sun-Earth line. This simple method is sufficient for our study, as the timing inaccuracies

it introduces are much shorter than the time scales of the GCR features we observe.

3. Event Selection

[27] Our goal is to discover whether a passing ICME and its shock inevitably lead to a two-step FD. We select ICMEs from 4 February 1998 to 31 December 2006 using the catalog created by *Cane and Richardson* [2003] and updated online (http://www.srl.caltech.edu/ACE/ASC/DATA/level3/icmetable2.htm#%28b%29). SWEPAM and MAG becoming simultaneously operational determines the starting date of our study.

[28] To create the catalog, the authors compare observed solar wind proton temperatures with those expected for "normally expanding" solar wind [*Burlaga and Ogilvie*, 1973]. Because ICMEs typically overexpand [*Richardson and Cane*, 1995], the authors search for times when the IPM has temperatures lower than expected. They then look by eye for reductions in field fluctuations, an increase in field organization, and discontinuities bounding the period in question.

[29] From their catalog, we select only ICMEs that have inferred shocks and have sheaths lasting at least 4 h. The latter criterion is the shortest a sheath can be while still having two clear steps in the hourly-averaged GCR data (see section 4.1 for our definition of a step). We exclude events during which solar energetic particles contaminate the neutron monitor observations. Applying these criteria produces 233 candidate events.

[30] Next we use the four Bartol neutron monitors (McMurdo, Newark, Thule, and South Pole) to select the ICMEs that drive GCR decreases $\gtrsim 1\%$ in at least two of the four monitors. Of the 233 candidates, 80 events meet this criterion. We also analyze two additional ICMEs that have sheaths shorter than 4 h because higher time resolution GCR data from SPI are available.

[31] Our method of selecting of events, while qualitative, is sufficient for this study. If the traditional understanding of two-step FDs is correct, then the selected events will clearly display that profile. We also expect the profiles to be somewhat variable, depending on each event's conditions. If the selected ICMEs do not, however, create two steps, then the model requires revision.

4. Analysis

4.1. Table of Events

[32] We chronologically list the selected events in Table 2. Each entry has the date and time of the shock arrival at Earth, unless otherwise marked, and the ICME arrival at ACE according to the catalog of *Cane and Richardson* [2003]. The ninth column shows the maximum magnetic field strength during the event. This value can be in either the sheath or the ICME. The tenth column lists the percentage of decrease as observed by the neutron monitor at McMurdo station. The fifth, sixth, and seventh columns indicate whether a step occurred at the shock, in the sheath, or at the leading edge of the ICME.

[33] The eighth column requires some explanation. In it, we indicate whether a local GCR recovery occurred in the sheath. This is a phenomenon to which little attention has been paid in

FD studies. For example, some events had a decrease beginning at the shock, a subsequent slight increase in the profile, and then another decrease. The recovery was generally to less than the predecrease GCR level. In other words, the recovery still appeared as part of the overall decrease in the GCR intensity.

[34] The eleventh shows the availability SPI data. Because INTEGRAL launched in October 2002 and SPI shuts down during solar energetic particles events, only five events are available. If the sheaths of these events lasted longer than 4 h, we enter in the table the results of the neutron monitor data. Otherwise, we leave blank the events' step entries (events 60 and 68).

[35] We consider a step to occur at an IPM feature, i.e., a shock or leading edge of an ICME, if the beginning of that step took place within 2 h of that feature in more than half the available neutron monitor time series. In other words, we search for GCR features that are isotropic: present at nearly the same universal time in the majority of neutron monitors. A short-lived feature that occurs in no more than a few neutron monitors of similar asymptotic longitudes is anisotropic. A longer-lived anisotropic feature will appear in a majority of neutron monitors, but at roughly a single local time. Its universal timing will shift with the asymptotic longitude of the monitor. Our criterion excludes both types of anisotropic features.

[36] Our definition of a step means that the shortest time a sheath can last while still having two clear steps in the hourly-averaged GCR data is 4 h. The definition of a step is somewhat qualitative; therefore we include all but the most insignificant steps, such as small ones immediately followed by an increase. The data from the various monitors tend to agree about the presence of a step to within only a couple hours. We finally note that our definition of a step does not require the GCR intensity subsequently to level. Thus, a step may mark the beginning of a decrease, and another step may occur if that decrease becomes steeper.

[37] For 7 events (25, 46, 48, 64, 65, 72, 78), data gaps in the ACE solar wind velocity data inhibit ballistically propagating the IMF data to Earth. In such cases, we instead use the maximum ICME speed from the list of *Cane and Richardson* [2003] to estimate the propagation time. While the actual speed during an event is variable, this estimate is sufficient to identify the timing of GCR features within the sheath.

4.2. Features of the Events

[38] We begin by describing some of the general features of the events. First, 73 of the 80 decreases begin at the shock. We must remember, however, that the actual number is 73 out of 233 events. Less than one third of the ICMEs with inferred shocks in the above catalog have a decrease. Of those with FDs, most begin at the shock. Fewer of the steps occur at the ICME (37 events), and even fewer within the sheath (22 events). Finally, 29 events have only one step, 25 of which occur at the shock.

[39] Only 13 are strictly traditional two-step FDs according to our analysis. In other words, they have steps only at the shock and the leading edge of the ICME, and they lack local increases within the sheath. Of these, six are poor events (events 35, 37, 44, 49, 57, and 70). Events 44 and 57 have significant anisotropic increases whose timings depend on the look direction of the neutron monitors. During the other

Table 2. Forbush Decreases From 4 February 1998 to 31 December 2006

Event	Disturbance Time[a,b] (UT)	ICME Start[a,c] (UT)	ICME End[a,c] (UT)	Shock Step	Sheath Step	ICME Step	Sheath Increase	Maximum B (nT)	FD Magnitude[d] (%)	S/C Data
				1998						
1	05/01 2156	05/02 0500	05/04 0200	x	–	–	–	21	6	–
2	05/04 0215(A)	05/04 1000	05/07 2300	x	–	–	–	45	3	–
3	06/13 1925	06/14 0400	06/15 0600	x	–	–	–	13	1	–
4	07/05 0315(A)	07/06 0600	07/09 0700	x	–	–	–	14	4	–
5	08/10 0046	08/10 1100	08/10 2200	x	–	–	–	12	2	–
6	08/26 0651	08/26 2200	08/28 0000	x	–	–	x	28	6	–
7	09/24 2345	09/25 0600	09/26 1600	x	x	–	x	43	13	–
8	10/18 1952	10/19 0400	10/20 0700	x	–	–	–	28	2	–
9	11/08 0451	11/09 0100	11/11 0100	x	x	–	x	38	6	–
10	12/28 1826	12/29 1800	12/31 0200	–	x	–	x	16	1	–
				1999						
11	01/22 1950(A)	01/23 0900	01/23 1800	x	–	x	x	20	7	–
12	02/18 0246	02/18 1000	02/20 1700	x	–	x	x	30	5	–
13	04/20 1600	04/21 0400	04/22 1400	x	–	–	–	14	2	–
14	06/26 2016	06/27 2200	06/29 0400	x	–	–	x	26	3	–
15	07/02 0059	07/03 0500	07/06 0600	x	–	–	x	12	1	–
16	07/26 2333(A)	07/27 1700	07/29 1200	x	–	–	x	8	2	–
17	10/21 0225	10/21 0800	10/22 0700	x	–	–	–	37	2	–
				2000						
18	02/11 0258	02/11 1600	02/11 2000	x	–	–	x	12	2	–
19	02/11 2352	02/12 1200	02/13 0000	x	–	–	–	26	3	–
20	02/20 2139	02/21 0500	02/22 1200	x	–	–	x	21	2	–
21	04/06 1639	04/07 0600	04/08 0600	x	–	–	x	34	4	–
22	05/23 2342	05/24 1200	05/27 1000	x	–	–	x	38	2	–
23	06/04 1502	06/04 2200	06/06 2200	x	–	x	x	14	3	–
24	07/13 0942	07/13 1300	07/14 1500	x	–	x	–	27	7	–
25	07/15 1437	07/15 1900	07/17 0800	x	–	x	x	60	10	–
26	07/19 1527	07/20 0100	07/21 0800	x	–	–	x	15	4	–
27	08/10 0501	08/10 1900	08/11 2100	–	–	–	x	15	3	–
28	08/11 1845	08/12 0500	08/13 2200	x	–	x	x	34	1	–
29	09/17 1657(A)	09/17 2100	09/21 0000	x	–	x	x	42	6	–
30	10/12 2228	10/13 1600	10/14 1700	x	x	–	x	22	3	–
31	10/28 0954	10/28 2100	10/29 2200	x	–	x	x	21	7	–
32	11/06 0948	11/06 1700	11/08 0300	x	x	–	x	25	7	–
33	11/26 1158	11/27 0800	11/28 0300	x	–	–	x	31	6	–
				2001						
34	01/23 1048	01/24 0900	01/26 0700	x	–	–	–	15	3	–
35	03/19 1114	03/19 1700	03/22 0000	x	–	x	–	22	3	–
36	03/31 0052	03/31 0500	03/31 2200	x	–	x	x	73	4	–
37	04/08 1101	04/08 1400	04/09 0400	x	–	x	–	23	7	–
38	04/11 1343	04/11 2200	04/13 0700	x	x	x	x	43	11	–
39	04/21 1601	04/21 2300	04/23 0300	–	–	–	–	16	2	–
40	04/28 0501	04/28 1400	05/01 0200	x	x	x	x	29	8	–
41	05/27 1459	05/28 0300	05/31 1400	x	–	–	x	15	4	–
42	08/03 0716	08/03 1100	08/03 1400	–	–	–	–	18	1	–
43	08/17 1103	08/17 2000	08/19 1600	x	x	x	x	34	7	–
44	08/27 1952	08/28 0000	08/29 2000	x	–	x	–	22	6	–
45	10/11 1701	10/12 0400	10/12 0900	x	x	–	–	29	6	–
46	11/06 0152	11/06 1200	11/09 0600	x	x	x	x	26	9	–
47	11/19 1815	11/19 2200	11/21 1300	x	–	x	–	15	2	–
48	11/24 0656	11/24 1400	11/25 2000	x	–	x	x	73	8	–
				2002						
49	03/18 1322	03/19 0500	03/20 1600	x	–	x	–	24	4	–
50	03/23 1137	03/24 1200	03/25 2000	x	x	x	x	13	3	–
51	04/17 1107	04/17 1600	04/19 1500	x	x	–	–	34	5	–
52	05/23 1050	05/23 2000	05/25 1800	x	x	–	x	63	6	–
53	07/19 1450(A)	07/20 0200	07/22 0600	x	–	–	x	21	4	–
54	08/18 1846	08/19 1200	08/21 1400	x	–	x	x	18	5	–
55	09/07 1636	09/08 0400	09/08 2000	x	x	–	x	27	4	–
56	11/16 2305(A)	11/17 1000	11/19 1200	–	–	x	–	12	7	–
				2003						
57	02/01 1305(A)	02/01 1900	02/03 0700	x	–	x	–	14	4	–
58	02/17 2150(A)	02/18 0400	02/19 1600	x	–	x	x	17	2	–
59	03/20 0420(A)	03/20 1200	03/20 2200	–	–	x	x	16	2	–
60	05/09 0455(A)	05/09 0700	05/11 0000					14	3	x

Table 2. (continued)

Event	Disturbance Time[a,b] (UT)	ICME Start[a,c] (UT)	ICME End[a,c] (UT)	Shock Step	Sheath Step	ICME Step	Sheath Increase	Maximum B (nT)	FD Magnitude[d] (%)	S/C Data
61	05/29 1825(A)	05/30 0200	05/30 1600	x	x	–	x	37	4	–
62	08/17 1421	08/18 0100	08/19 1500	x	–	x	x	28	2	–
63	10/24 1524	10/24 2100	10/25 1200	x	x	x	x	36	6	x
64	10/29 0611	10/29 1100	10/30 0300	x	–	x	x	68	24	–
65	10/30 1619(A)	10/31 0200	11/02 0000	x	–	x	x	42	7	–
					2004					
66	01/22 0137	01/22 0800	01/23 1700	x	–	x	–	30	9	x
67	07/24 0613	07/24 1400	07/25 1500	x	x	–	x	25	4	–
68	07/26 2249	07/27 0200	07/27 2200					26	15	x
69	09/13 2003	09/14 1500	09/16 1200	x	x	x	x	31	5	–
70	11/07 1827	11/07 2200	11/09 1000	x	–	x	–	63	8	–
					2005					
71	02/17 2200	02/18 1400	02/19 0600	x	x	–	x	24	2	–
72	05/15 0238	05/15 0600	05/19 0000	x	–	x	–	56	10	–
73	05/29 0905(A)	05/30 0100	05/30 2300	x	–	–	x	23	4	–
74	06/12 0700	06/12 1500	06/13 1300	x	–	–	–	26	3	–
75	07/10 0250(A)	07/10 1000	07/12 0400	x	–	x	x	26	4	–
76	07/17 0055(A)	07/17 1400	07/18 2300	x	–	x	x	15	4	–
77	09/02 1300	09/2 1800	09/3 0400	x	–	–	–	18	3	
78	09/11 0114	09/11 0500	09/12 0700	x	x	–	–	27	13	–
					2006					
79	04/13 1100	04/13 1500	04/14 0700	x	–	x	–	20	2	–
80	07/09 2136	07/10 2100	07/11 1900	x	x	–	x	10	5	
81	08/19 1055(A)	08/20 1300	08/21 1600	–	x	–	–	21	4	x
82	12/14 1414	12/14 2200	12/15 1300	x	–	x	x	21	8	–

[a]These times (MM/DD HHMM) are from *Cane and Richardson* [2003], as updated by the online version of their catalog (http://www.srl.caltech.edu/ACE/ASC/DATA/level3/icmetable2.htm#%28b%29).

[b]This is the time of the geomagnetic storm sudden commencement when present. Otherwise, the time of shock passage at ACE is given and labeled by "(A)."

[c]This is the time at ACE.

[d]This is the depth of the FD at the McMurdo neutron monitor.

four events, few of the neutron monitors clearly show the two-step profile. Instead, some show only the first step, and others show the second. Thus, the two-step profile is only apparent by looking at all the neutron monitors. The other seven traditional two-step FDs (events 24, 40, 51, 64, 68, 72, 79), however, are better examples. Event 64, shown in Figure 1, is the clearest of these. Note that although the decrease begins before the shock, the time difference is less than the 2 h we use to determine concurrency. Event 66, however, changes its categorization when observed with the SPI data, as we describe in section 4.3.

[40] Twenty-three events are nontraditional two-step FDs. In addition to the two steps, these events have either just an increase in the sheath (15 events) or both an increase and a third step in the sheath (7 events). We will discuss these in more detail in section 5. Suffice to say that these events suggest the presence of additional processes that are lacking in the traditional model.

[41] Even though we choose these ICME events as the most likely to create two-step FDs, the majority (43 of 80) lack steps at both the shocks and the ICMEs. 25 of these had steps only at the shock, 2 had steps only in the sheath, 2 had steps only at the ICME, and 13 had steps at the shock and in the sheath. None had steps in the sheath and at the ICME. Also, 3 events had significant anisotropic features which prevented identification of steps. Finally, 50 events had increases within the sheath.

4.3. SPI Observations

[42] The analysis in section 4.2 compares hourly GCR data with 16 s unpropagated or 64 s propagated IMF data. This difference in resolution between the GCR and IMF data sets inhibits making reliable associations between features in the two. Using the high time resolution of the space-based GCR data enables a better comparison. Because SPI is a relatively new yet powerful instrument for observing GCRs, we will look in detail at each available event.

[43] The first is event 60, shown in Figure 2. The FD shows only one step that begins about half an hour after the shock passes. A small second step may exist at the leading edge of the ICME, despite the presence of a strong tangential discontinuity.

[44] Since there is no immediately obvious cause to initiate the FD at that time, we analyze the sheath for evidence of planar magnetic structure (PMS), as *Jordan et al.* [2009] found that such structure can initiate a decrease. A PMS forms when a disturbance compresses the IMF or causes the field to drape around the disturbance [*Nakagawa et al.*, 1989; *Neugebauer et al.*, 1993]. The IMF vector remains in the same plane even while significantly rotating. PMSs often occur between ICMEs and their shocks [*Jones and Balogh*, 2000]. We find a region labeled in Figure 2 that coincides with the start of the FD. To discover the planarity of the region, we use the minimum variance analysis described by *Sonnerup and Scheible* [2000]. The mid to minimum eigen-
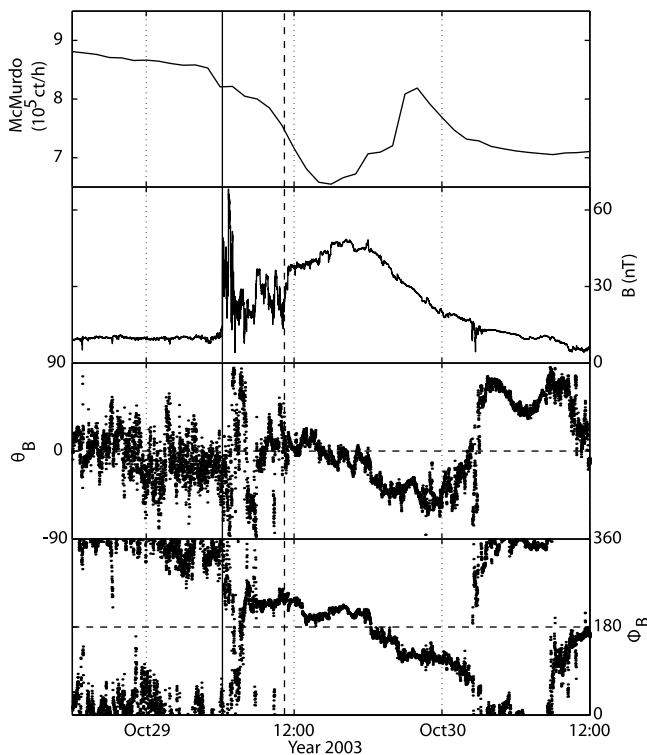
Figure 1. The first panel shows galactic cosmic ray (GCR) data from McMurdo during event 64. The second, third, and fourth panels show magnetic field strength and angular coordinates of the field direction. θ_B is the interplanetary magnetic field (IMF) vector's latitude with respect to the ecliptic plane, and ϕ_B is its angle in the ecliptic plane with respect to the Sun-Earth line. We propagate the data using maximum interplanetary coronal mass ejections (ICME) speed (1900 km/s) from *Cane and Richardson* [2003]. The vertical solid line marks the shock's arrival at Earth, and the vertical dashed line marks the arrival of the ICME.

value ratio during the PMS is 6, which means that the field was planar. As we discuss below, the concurrence of the PMS and the beginning of the FD indicates that the former may have initiated the latter.

[45] The second event is 63 (see Figure 3). The ICME's sheath was long enough to allow analysis with the neutron monitor data, which evidenced steps at the shock, in the sheath, and at the IMCE. The higher-resolution data show, however, that the decrease did not begin until almost an hour after the shock had passed. As with the previous event, we find a PMS (mid to minimum eigenvalue ratio of 5) that begins after the shock but is concurrent with the initiation of the FD. We also note that the local maximum in the GCR time series is present in both the SPI and neutron monitor data. It occurs at the leading edge of what could be an ICME, although it is unlisted in the catalog of *Cane and Richardson* [2003]. While the region has a relatively high proton temperature, the magnetic field variance is low. The GCR intensity decreases throughout the feature into the interaction region between it and the cataloged ICME. The interaction region also contains a PMS with a mid to minimum eigenvalue ratio of 5. A slight step is visible in the GCR time series upon entry into the ICME.

[46] Third is event 66 (see Figure 4). According to our analysis with neutron monitor data, this event is a traditional two-step FD. The SPI data, however, show that it is actually somewhat different. The decrease begins at the shock, and then the GCR intensity subsequently begins to level. A second step occurs almost an hour before the arrival of the ICME. That step coincides with a period of PMS (mid to minimum eigenvalue ratio of 6), not with the ICME as in the neutron monitor analysis. We note that, as in event 63, there appear to be two ICMEs separated by an interaction region of more turbulent IMF. *Cane and Richardson* [2003] mark the first but miss the second, which begins with a significant tangential discontinuity. The latter ICME may have created a small GCR step.

[47] The fourth is event 68 (see Figure 5). The sheath was too short to analyze with the neutron monitor data. Despite the strength of the shock, the SPI data display only a slight decrease beginning at the shock. The step at the leading edge of the ICME is more clear. For completeness, we do search for but find no evidence of a PMS.

[48] The final event is 81. As *Jordan et al.* [2009] analyzed this event in detail, we do not show it here. The FD does not begin at the shock in either the ground- or space-based data. The neutron monitors indicate the decrease begins at the ICME, but the SPI data show instead that it begins in the PMS preceding an uncatalogued ICME. The
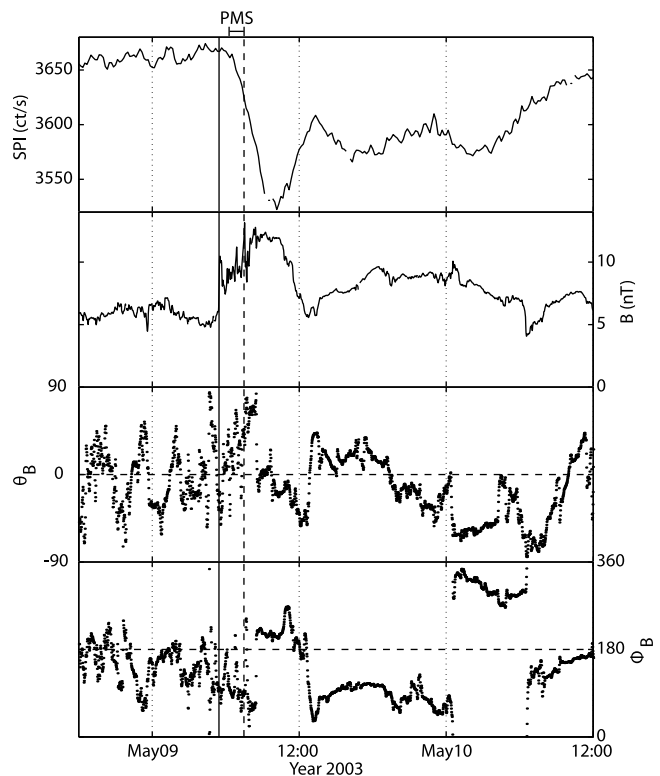

Figure 2. The first panel shows the GCR data from the Spectrometer for INTEGRAL (SPI) during event 60. The second, third, and fourth panels show magnetic field strength and angular coordinates of the field direction. The IMF data are ballistically propagated. The vertical solid line marks the shock's arrival at ACE, and the vertical dashed line marks the arrival of the ICME.
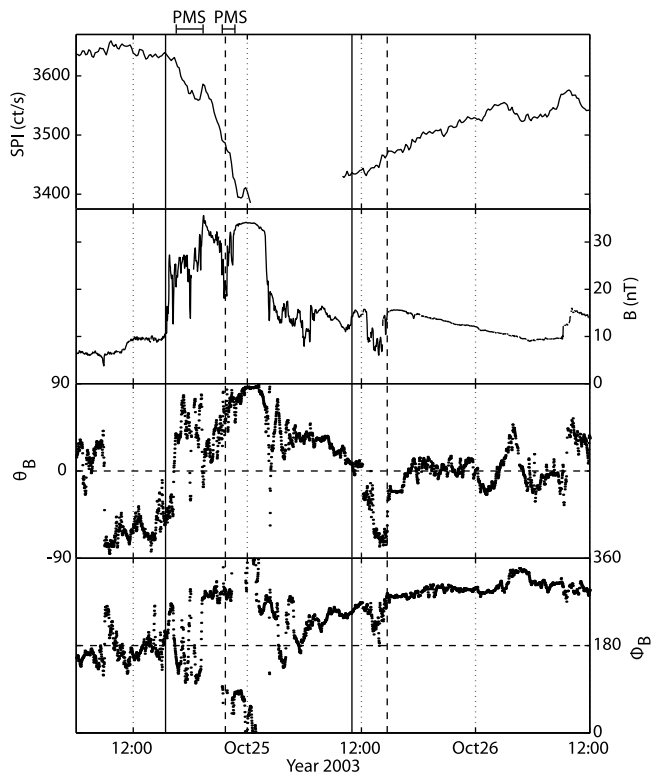
Figure 3. The first panel shows the GCR data from SPI during event 63. The large data gap occurred when INTEGRAL passed through Earth's radiation belts. The second, third, and fourth panels show magnetic field strength and angular coordinates of the field direction. The IMF data are ballistically propagated. The vertical solid line marks the shock's arrival at Earth, and the vertical dashed line marks the arrival of the ICME.

PMS had a mid to minimum eigenvalue ratio of 20. The decrease profile had three steps, the first two of which were associated with a rapidly rotating IMF. The third step was concurrent with the arrival of the first ICME. The second, cataloged ICME also created a step in the GCR intensity by interrupting its recovery.

[49] The discrepancy between the ground- and space-based data provides clear examples of how both the number and timing of steps depends on the temporal resolution of the data. As to be expected, the higher-resolution GCR data show complexity that is invisible at lower resolutions. Additionally, the resolution enables us to make better associations between IMF and GCR features. The 4 h windows that we use to identify steps in the neutron monitor data introduce large uncertainties in determining the concurrency of features. The higher-resolution GCR data remove this ambiguity and reveal an unexpected concurrence of PMS and GCR decreases.

[50] To summarize, the high time resolution data from SPI present a more complex picture of FDs. In four of the five events for which spacecraft data are available, the FD began after the arrival of the shock. Also, four of the observed steps were concurrent with PMS, rather than a shock or an ICME. Finally, in events that we can also analyze the

neutron monitors (events 63, 66, and 81), the timing and profile of the decrease changes when we use the SPI data.

5. Discussion

5.1. Lack of Two-Step FDs

[51] The most surprising result of the above analysis is the lack of two-step FDs. The traditional FD model predicts that all the events included in this study would have two clear steps: one beginning at the shock and the other at the leading edge of the ICME. 233 candidate ICMEs had inferred shocks, yet only 81 of them created FDs. (This contradicts the assertion of *Cane and Richardson* [2003] that a decrease in the GCRs typically accompanies ICMEs.) Of these, only 13 created two-step FDs. Furthermore, only 6 of these two-step events were clear in multiple neutron monitors. The other 7 either showed a strong anisotropic component interfering with the observations or can only be seen to be two-step events by combining disparate time series.

[52] A few possible explanations exist for this discrepancy between the model and the observations. The first possibility is that the event boundaries are incorrect. That is, perhaps some of the 233 events improperly mark ICMEs. The 82 events included in this study, however, all qualitatively appear to be ICMEs, especially in the magnetic field
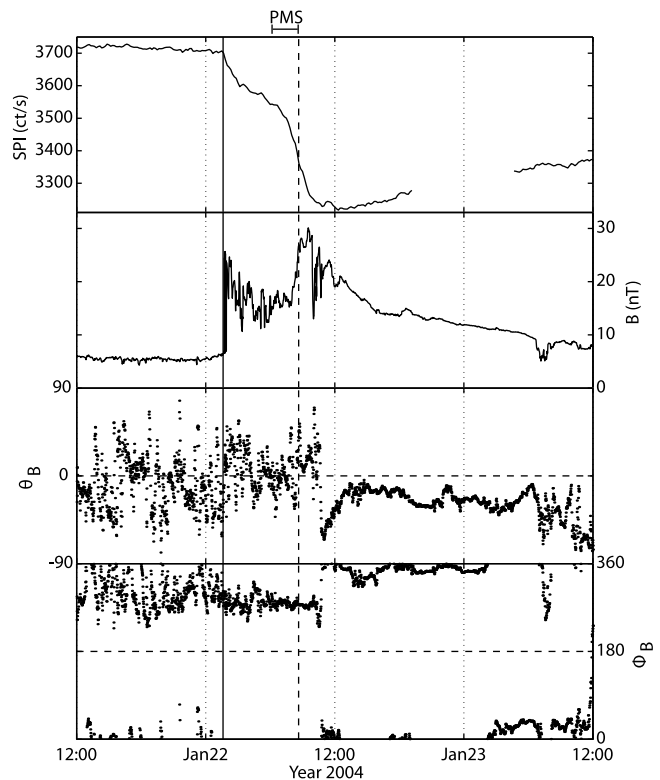

Figure 4. The first panel shows the GCR data from SPI during event 66. The large data gap occurred when INTEGRAL passed through Earth's radiation belts. The second, third, and fourth panels show magnetic field strength and angular coordinates of the field direction. The IMF data are ballistically propagated. The vertical solid line marks the shock's arrival at Earth, and the vertical dashed line marks the arrival of the ICME.
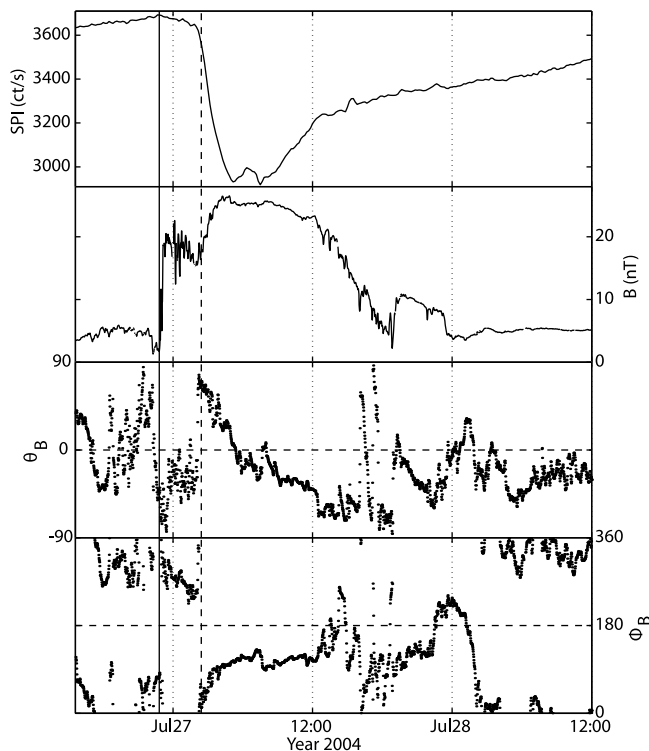
Figure 5. The first panel shows the GCR data from SPI during event 68. The second, third, and fourth panels show magnetic field strength and angular coordinates of the field direction. The IMF data are ballistically propagated. The vertical solid line marks the shock's arrival at Earth, and the vertical dashed line marks the arrival of the ICME.

data. Since the IMF controls the GCRs, this magnetic signature would be the main indicator of whether the GCRs would be modulated in accordance with the model. The 4 h window we use for defining steps also makes sure that even if the boundaries are somewhat incorrect, they will not influence our analysis. Thus, this first possibility seems unlikely.

[53] A second possibility is that the two-step model works only for "ideal" ICMEs, e.g., those similar to that in event 64, shown above in Figure 1. Indeed, such events are likely to have steps that our analysis associates with the shock and the ICME. Yet these events can also have extra steps or increases in the sheath (events 25, 46, 48, and 82). Event 48, shown in Figure 6, is a good example of an "ideal" ICME that created something other than a traditional two-step FD. The decrease begins with the shock but then recovers even while the IMF remained turbulent, although at a lower field strength (we discuss similar recoveries below in section 5.4). The GCRs decrease again at the ICME's arrival. Event 60 is another example of a "classic" ICME (see Figure 2). The SPI data, however, show that the decrease had only one step, which began in the sheath. Thus, this possible explanation for the lack of two-step FDs also appears to be unlikely.

[54] Another possibility is that FDs may depend on nonlocal conditions that are poorly represented by in situ IPM observations. Because of their relativistic speeds and large gyroradii with respect to solar wind particles, GCRs are

affected by both local and nonlocal conditions. The regions from which the GCRs arrive at the detector can also modulate the intensity of cosmic rays within the sheath without affecting in situ IPM data. This is a difficult scenario to analyze, however. We discuss related processes in sections 5.2 and 5.4.

[55] In addition to discovering a lack of two-step FDs, we find that 29 events have one step. According to the FD model, though, one-step FDs should occur in only two scenarios. The first occurs when a shock but not its ICME passing the GCR detector, and the second when an ICME without a shock passing the detector. Yet all of the events in this study have both shocks and ICMEs. This suggests that it is impossible identify the type of ICME using FDs profiles. Also, 25 of the one-step FDs begin at the shock and thus lack a step at the leading edge of the ICME. We discuss such events when we discuss ICME-associated steps in section 5.3.

[56] We also find 7 FDs with three steps. The second step, the one inside the sheath, is always associated with a local increase in the GCR intensity. We note that they only occur in sheaths with evidence of magnetic structure, so we discuss them in section 5.4. Also, we find no FDs with more than three steps. Part of the reason may be due to some of the sheaths being too short to identify more steps.
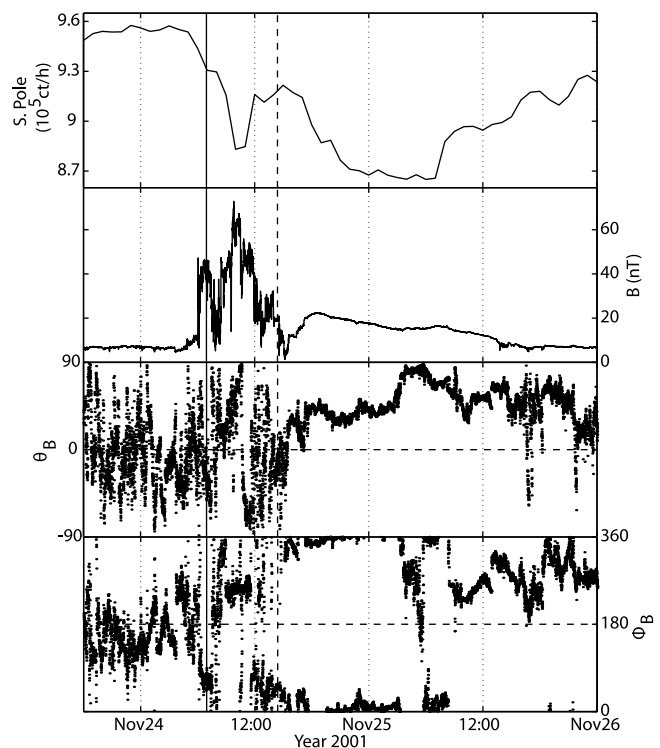

Figure 6. The first panel shows the GCR data from the South Pole during event 48. The second, third, and fourth panels show magnetic field strength and angular coordinates of the field direction. We propagate the data using the maximum ICME speed (1040 km/s) from [*Cane and Richardson*, 2003], but the shock's time is still an hour earlier than that listed by *Cane and Richardson* [2003]. The vertical solid line marks the shock's arrival at Earth, and the vertical dashed line marks the arrival of the ICME.

[57] The lack of two-step FDs and the occurrence of both one- and three-step FDs all contradict the predictions of the traditional FD model. This discrepancy is not just the result of the variety of ICMEs and their sheaths; even seemingly similar ICMEs can lead to different FD profiles. We seek now to explore in more detail the possible causes of the variety of profiles.

5.2. Steps Associated With Shocks

[58] The traditional model of FDs does, for the most part, correctly predict the relation of shocks and FDs, but only when GCR decreases do occur; 73 of the 80 decreases begin at the shock. The shock thus appears to play an important role in events that decrease the GCR intensity. Events that lacked steps at the shock either had interference from an anisotropic component or had weaker shock strengths.

[59] We note that the association between shocks and the start of a FD is only true, however, at an hourly resolution and with the 4 h window we used to define concurrence. The SPI data suggest the situation may be different at higher time resolutions. Of the five events with SPI data, only event 66 shows a clear decrease beginning at the shock (see Figure 4). The others imply that the shock may not be as impenetrable to the GCRs as suggested by the model.

[60] Shock conditions can vary over the shock front. For example, *Neugebauer and Giacalone* [2005] observed nonplanar distortions in interplanetary shocks. They found the average curvature at 1 AU to be ~3×10^6 km or about an order of magnitude greater than the gyroradii of the lowest-energy GCRs we use in this study. These spatially variable conditions along the shock front can create large spatial variations in the intensity of energetic particles (see simulation results in Figure 1 of *Neugebauer and Giacalone* [2005]). GCRs, although possessing higher energies than the simulated population, may similarly penetrate some regions of the shock front more easily than others. Perhaps they can more easily penetrate the sheath through quasi-parallel areas of the shock front. Further research is needed to address this.

5.3. Steps Associated With ICMEs

[61] ICMEs, according to the traditional FD model, should create steps in GCRs. In less than half of the events, however, does the leading edge of the ICME create an obvious step in the GCRs. At first glance this appears to suggest that ICMEs are less effective than shocks at decreasing cosmic rays. Such a suggestion would contradict work showing that both contribute about equally to the overall FD [*Wibberenz et al.*, 1998].

[62] The suggestion is incorrect, though, because the effectiveness of a decrease is unrelated to the presence of a step. In ~90% of all 80 events, the decrease continues into the ICME, even if no step were apparent. Therefore, the observations do agree with part of the model: the ICME does contribute to the decrease. On the other hand, the observations contradict the model by showing that a FD is more likely to have no step at an ICME's leading edge.

[63] Even during FDs that seem to have steps at the ICME, care must be used when making associations with hourly resolution data and 4 h windows. Event 66 in the ground data appears to be a classic two-step event (see Figure 4). The SPI data show, however, that the second step

occurred began over an hour before the arrival of the ICME. Event 81, described above, shows that while the neutron monitor data indicate that the step began at the ICME, the SPI data show that it actually began more than an hour before the ICME arrival. Firm assertions of the concurrence of features are unreliable when the resolutions of the two data sets are too different.

5.4. Structure in the Sheath

[64] The traditional FD model predicts two GCR steps with no increases between. Yet in over half the events, the GCRs increase locally within the sheath. A similar phenomenon has been noted in ICMEs [*Nagashima et al.*, 1990] but not in the sheaths. The increases are local for two reasons. First, they are superposed on the overall FD; the decrease continues after the increase. Second, the increases are generally to levels less than the GCR intensity before the FD. Since some increases are due to anisotropic features in the cosmic rays, however, we restrict this discussion to increases that are isotropic and thus easier to relate to IMF features.

[65] A model dependent on turbulence alone (see, for example, the simple one-dimensional model of *Wibberenz et al.* [1998]) cannot account for a local increase. To create local increases, the sheath must contain structure that separates the regions of lower GCR intensity from the local maximum. For example, one possibility is that the increase could be due to a cosmic ray "conduit." This is similar to suggestions by *Bartley et al.* [1966] and *Borovsky* [2008]. Perhaps the region of local increase connects to another region closer to the shock front and thus possessing a greater GCR intensity. The higher intensity could then propagate through the conduit and create the local increase.

[66] Event 82, shown in Figure 7, may show evidence for such a situation. The GCR flux increases just before the arrival of the ICME. The increase appears associated with a feature in the IMF data. We observe no PMS during the increase. While the direction of the IMF was variable during this time, the region is bounded by lower magnetic field. While the exact mechanism is unclear, this event indicates that structure within the sheath can play an important role in the determining the GCRs' decrease profile.

[67] We also note that in some cases structure in the sheath can create a leveling out between steps, such as those seen in the work by *Cane et al.* [1994] and *Wibberenz et al.* [1998], as mentioned in section 1.2. Event 31, shown in Figure 8, is a good example of this. The decrease has two steps, one at the shock and the other at the ICME, and a slight increase at the leading edge of the ICME. The sheath contains a feature that resembles a flux rope, a region with a relatively low field strength variance and a relatively smooth rotation in the field direction. The flux rope is approximately concurrent with a period of constant GCR intensity. Thus, in this event, the two-step profile is the product of a coherent structure, not turbulence as suggested by the model. Important structure like this flux rope can remain unresolved in hourly resolution data.

[68] As we mentioned above in relation to the events observed with SPI, planar magnetic structures also appear to play an important role in decreasing the GCR intensity. *Intriligator et al.* [2001] describe how flow shears can decrease cross-field transport. Unfortunately, the lower
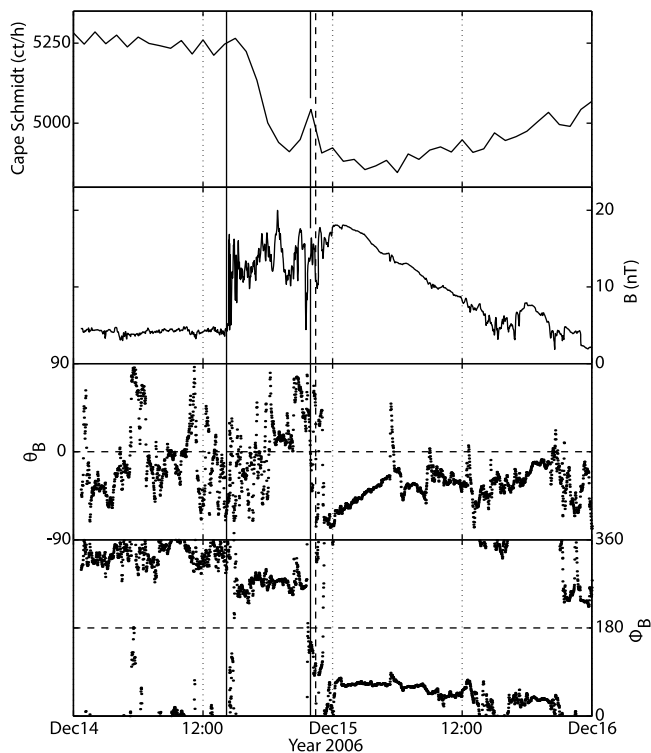
Figure 7. The first panel shows the GCR data from Cape Schmidt during event 82. The second, third, and fourth panels show magnetic field strength and angular coordinates of the field direction. The IMF data are ballistically propagated. The first vertical solid line marks the shock's arrival at Earth, the second marks the GCR increase, and the vertical dashed line marks the arrival of the ICME.

resolution of the neutron monitor data makes it difficult to determine how important PMSs may be to FDs in general. This is a topic worth further research.

5.5. Categorizing FDs

[69] The above discussion shows that describing FDs as one- or two-step events is insufficient for the majority of FDs. The categorization is ambiguous because the number of steps can depend on the resolution of the data being used. It also ignores the small-scale IMF structure that can create unexpected profiles. Therefore, the model is too idealized to explain the variety of FDs that are driven by equally varied ICMEs.

[70] The variety of FD profiles suggests that structure within the sheath determines the FD profile, i.e., the number of steps in the decrease and the presence of local recoveries. The presence of turbulence may explain decreases in the sheath, but only structure can explain the increases. Each sheath, then, has a unique combination of turbulence and structure that leads to a unique decrease profile. Thus, the number of steps relates to the uniquely specific conditions of a given event.

[71] It is thus necessary to discard the traditional classification scheme. Each FD must be studied as a unique event in the detailed context of its driving interplanetary conditions. Only this enables the discovery of generalizations describing

the variety of events. We have shown in this study that such generalizations must focus not on the FD profiles themselves but on the cause of the profiles. Our work represents a step from what is fundamentally a phenomenological classification of FDs to one that is causal.

6. Conclusions

[72] In this work we test the traditional model describing the formation of FDs in GCR intensity. The model states that if an ICME and its shock encounter a GCR detector, that detector will record a two-step FD. If only a shock or only an ICME encounter the detector, it will record a one-step FD. To test the model, we search for ICMEs that should create two-step decreases and explore whether they do so. We conclude the following:

[73] 1. Contrary to the model and to the study of *Cane et al.* [1996], ICMEs with shocks do not necessarily create two-step FDs. Of the 233 ICME events that had sheaths long enough for this study, only 80 created FDs. Of these, only 13 FDs had two steps. Even of these 13, only 7 were clearly two-step FDs in multiple neutron monitors. Furthermore, the high time resolution SPI data show that one of these (event 66) was not actually a two-step event. The reason for the lack of FDs is unknown and is important for future study.

[74] 2. The ICME events and their associated FDs possess profiles that are more varied than predicted by the model.
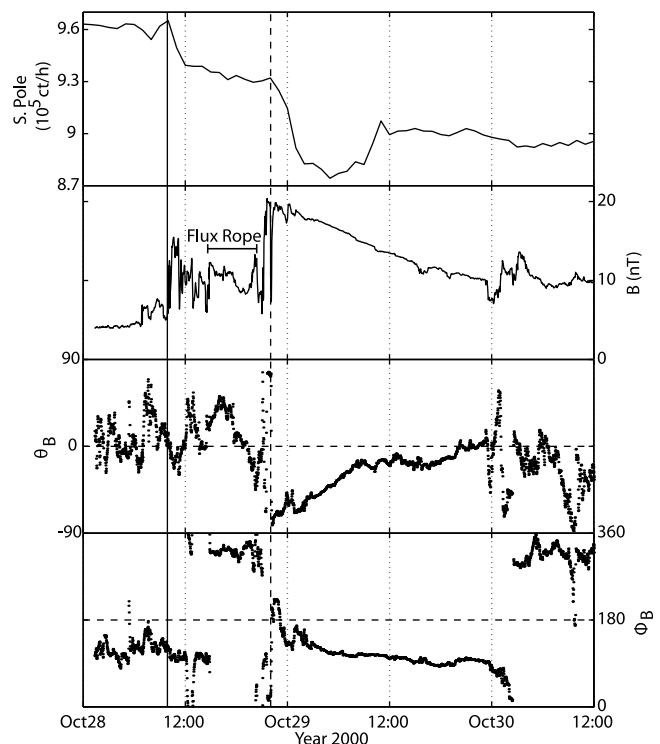

Figure 8. The first panel shows the GCR data from the South Pole during event 31. The second, third, and fourth panels show magnetic field strength and angular coordinates of the field direction. The IMF data are ballistically propagated. The vertical solid line marks the shock's arrival at Earth, and the vertical dashed line marks the arrival of the ICME. The flux rope is labeled.

Thus, using GCR data to determine whether both an ICME and its shock encounter the detector is impossible. All the events should have two steps, but we find events with one or three steps.

[75]   3. The high time resolution SPI data indicate that FDs are more complex than previously thought. They also highlight the limitations of comparing hourly GCR data with much higher resolution IPM data. The 4 h window we used because of the neutron data creates necessarily large uncertainties when associating GCR features with IMF features. High time resolution spacecraft data present an unexplored potential to probe processes on scales similar to those measured by IMF instruments.

[76]   4. The association between shocks and the beginning of FDs is clear. The SPI data and some neutron monitor data, however, show that FDs can sometimes start after the shock. This suggests that shock fronts may be permeable to an extent.

[77]   5. The leading edges of ICMEs are more likely to be associated with no GCR step than with one. Even so, they are effective at decreasing GCR intensity, since 90% of the FDs reach a minimum in the associated ICMEs.

[78]   6. Local GCR increases during ICME sheaths suggest that the traditional FD model ignores the importance of small-scale IMF structure. The increases indicate that a process other than pure IMF turbulence may be present. GCR "conduits" such as small IMF flux ropes may explain the regions of increased GCR intensity.

[79]   7. Generally ignored small-scale IMF structure, such as flux ropes or PMS, contribute to the variety of FD profiles. This is seen more clearly in the high time resolution SPI data. The different structures can create localized increases, localized decreases, or even levelings in the GCR time series.

[80]   8. The traditional one- or two-step classification of FDs is inadequate to explain our study. Each FD must be studied as a unique event in the detailed context of its driving interplanetary conditions. Only this method will lead to a truly causal classification scheme.

[81]   Much work remains to understand better the processes that create FDs. For example, our study did not test whether the possible role of turbulence agrees with the FD model's predictions. One open question is how to distinguish between GCR modulation due to turbulence and that due to structure. Another area needing continued study is the structure of shock fronts; this is also important for understanding how shocks can accelerate particles. The permeability of shocks to energetic particles may play a key role. Capitalizing on the high time resolution data from spacecraft and neutron monitors, e.g., the Neutron Monitor Database [*Mavromichalaki*, 2010], will help answer these questions.

References

Barnden, L. R. (1973), The large-scale magnetic field configuration associated with Forbush decreases, *Conf. Pap. Int. Cosmic Ray Conf. 13th*, *2*, 1277–1282.

Bartley, W. C., R. P. Bukata, K. G. McCracken, and U. R. Rao (1966), Anisotropic cosmic radiation fluxes of solar origin, *J. Geophys. Res.*, *71*(13), 3297–3304.

Borovsky, J. E. (2008), Flux tube texture of the solar wind: Strands of the magnetic carpet at 1 AU?, *J. Geophys. Res.*, *113*, A08110, doi:10.1029/2007JA012684.

Burlaga, L. F., and K. W. Ogilvie (1973), Solar wind temperature and speed., *J. Geophys. Res.*, *78*, 2028–2034, doi:10.1029/JA078i013p02028.

Cane, H. V. (1993), Cosmic ray decreases and magnetic clouds, *J. Geophys. Res.*, *98*, 3509–3512.

Cane, H. V. (2000), Coronal mass ejections and Forbush decreases, *Space Sci. Rev.*, *93*, 55–77, doi:10.1023/A:1026532125747.

Cane, H. V., and I. G. Richardson (2003), Interplanetary coronal mass ejections in the near-Earth solar wind during 1996–2002, *J. Geophys. Res.*, *108*(A4), 1156, doi:10.1029/2002JA009817.

Cane, H. V., I. G. Richardson, and T. T. von Rosenvinge (1993), Cosmic ray decreases and particle acceleration in 1978–1982 and the associated solar wind structures, *J. Geophys. Res.*, *98*, 13,295–13,302, doi:10.1029/93JA00955.

Cane, H. V., I. G. Richardson, T. T. von Rosenvinge, and G. Wibberenz (1994), Cosmic ray decreases and shock structure: A multispacecraft study, *J. Geophys. Res.*, *99*, 21,429–21,441.

Cane, H. V., I. G. Richardson, and T. T. von Rosenvinge (1996), Cosmic ray decreases: 1964–1994, *J. Geophys. Res.*, *101*, 21,561–21,572, doi:10.1029/96JA01964.

Coleman, P. J., Jr., C. P. Sonett, D. L. Judge, and E. J. Smith (1960), Some preliminary results of the Pioneer V magnetometer experiment, *J. Geophys. Res.*, *65*, 1856–1857.

Fan, C. Y., P. Meyer, and J. A. Simpson (1960), Rapid reduction of cosmic-radiation intensity measured in interplanetary space, *Phys. Rev. Lett.*, *5*, 269–271, doi:10.1103/PhysRevLett.5.269.

Forbush, S. E. (1937), On the effects in cosmic-ray intensity observed during the recent magnetic storm, *Phys. Rev.*, *51*, 1108–1109, doi:10.1103/PhysRev.51.1108.3.

Intriligator, D. S., J. R. Jokipii, T. S. Horbury, J. M. Intriligator, R. J. Forsyth, H. Kunow, G. Wibberenz, and J. T. Gosling (2001), Processes associated with particle transport in corotating interaction regions and near stream interfaces, *J. Geophys. Res.*, *106*, 10,625–10,634, doi:10.1029/2000JA000070.

Jones, G. H., and A. Balogh (2000), Context and heliographic dependence of heliospheric planar magnetic structures, *J. Geophys. Res.*, *105*, 12,713–12,724, doi:10.1029/2000JA900003.

Jordan, A. P., H. E. Spence, J. B. Blake, T. Mulligan, D. N. A. Shaul, and M. Galametz (2009), Multipoint, high time resolution galactic cosmic ray observations associated with two interplanetary coronal mass ejections, *J. Geophys. Res.*, *114*, A07107, doi:10.1029/2008JA013891.

Lockwood, J. A. (1971), Forbush decreases in the cosmic radiation, *Space Sci. Rev.*, *12*, 658–715, doi:10.1007/BF00173346.

Mavromichalaki, H., A. Papaioannou, C. Sarlanis, G. Souvatzoglou, M. Gerontidou, C. Plainaki, M. Papailiou, G. Mariatos, and NMDB Team (2010), Establishing and using the real-time Neutron Monitor Database (NMDB), *Astron. Soc. Pac. Conf. Ser.*, *424*, 75–80.

Morrison, P. (1956), Solar origin of cosmic-ray time variations, *Phys. Rev.*, *101*, 1397–1404, doi:10.1103/PhysRev.101.1397.

Nagashima, K., S. Sakakibara, K. Fujimoto, R. Tatsuoka, and I. Morishita (1990), Localized pits and peaks in Forbush decrease, associated with stratified structure of disturbed and undisturbed magnetic fields, *Nuovo Cimento C*, *13*, 551–587.

Nakagawa, T., A. Nishida, and T. Saito (1989), Planar magnetic structures in the solar wind, *J. Geophys. Res.*, *94*, 11,761–11,775.

Neugebauer, M., and J. Giacalone (2005), Multispacecraft observations of interplanetary shocks: Nonplanarity and energetic particles, *J. Geophys. Res.*, *110*, A12106, doi:10.1029/2005JA011380.

Neugebauer, M., D. R. Clay, and J. T. Gosling (1993), The origins of planar magnetic structures in the solar wind, *J. Geophys. Res.*, *98*, 9383–9389.

Richardson, I. G., and H. V. Cane (1995), Regions of abnormally low proton temperature in the solar wind (1965–1991) and their association with ejecta, *J. Geophys. Res.*, *100*, 23,397–23,412, doi:10.1029/95JA02684.

Sanderson, R. T., J. Beeck, G. R. Marsden, C. Tranquille, K. Wenzel, B. R. McKibben, and E. Smith (1990), A study of the relation between

magnetic clouds and Forbush decreases, *Conf. Pap. Int. Cosmic Ray Conf. 21st*, 6, 251–254.

Simpson, J. A. (1954), Cosmic-radiation intensity-time variations and their origin. III. The origin of 27-day variations, *Phys. Rev.*, 94, 426–440, doi:10.1103/PhysRev.94.426.

Simpson, J. A. (2000), The cosmic ray nucleonic component: The invention and scientific uses of the neutron monitor – (Keynote Lecture), *Space Sci. Rev.*, 93, 11–32, doi:10.1023/A:1026567706183.

Sonnerup, B. U. O., and M. Scheible (2000), Minimum and maximum variance analysis, in *Analysis Methods for Multi-spacecraft Data*, edited by G. Paschmann and S. J. Schwartz, *Eur. Space Agency Spec. Publ., ESA SP-449*, 185–220.

Wibberenz, G., J. A. Le Roux, M. S. Potgieter, and J. W. Bieber (1998), Transient effects and disturbed conditions, *Space Sci. Rev.*, 83, 309–348.

J. B. Blake, The Aerospace Corporation, 2310 E. El Segundo Blvd., El Segundo, CA 90245-4691, USA.

A. P. Jordan and H. E. Spence, Institute for the Study of Earth, Oceans, and Space, University of New Hampshire, Durham, NH 03824, USA. (a.p. jordan@unh.edu)

D. N. A. Shaul, High Energy Physics Group, Department of Physics, Imperial College London, London SW7 2AZ, UK.